

Variations of Color and Leachate Contents of Volcanic Ashes from Sakurajima Volcano, Japan

Isoji MIYAGI*, Hiroshi SHINOHARA* and Jun'ichi ITOH*

(Received September 20, 2011; Accepted June 20, 2012)

To understand magma degassing processes near the top of volcanic conduit, we investigated a series of volcanic ashes from the Sakurajima volcano, Japan. We describe temporal changes in the color and the amount of leachates (Cl, F, S) of ash erupted from 1981 to 2011. Based on the amount of leachates present, ash samples are classified into two major groups: one is with a molar S/Cl ratio of ~ 10 , and another with S/Cl of ~ 1 and that is relatively depleted in S. Ash samples that were erupted during 1981–1991 from the Minamidake summit crater belong to the latter group. Ashes erupted from the Showa crater in early 2008 belong the former group, of which the S content was found to decrease systematically through time, although in 2011, ashes of the latter group erupted for the first time from this crater. Based on coloration, the ash samples in this study are classified into two groups: one with a yellowish color, another with a less yellowish color. The coloration of the former group can be explained by the existence of yellowish native sulfur as well as other hydrothermally altered minerals. We observed positive correlations between the interval of successive eruptions and both the yellowness and the amount of ash leachates. Our interpretation is that the observed temporal changes in volcanic ash result from a transition in the amount of fumarolic sulfur accumulation in partly solidified magma near the top of volcanic conduit, which we interpret to reflect the mean residence time of the magma. The magma probably periodically renewed in response to ash eruption and/or magma convection near the top of the volcanic conduit.

Key words: Sakurajima; volcanic ash, color, volcanic gas, magma degassing, S, F, Cl

1. Introduction

Developing a sound understanding of magma degassing processes can ultimately yield clues to the mechanisms that cause volcanic eruptions (Eichelberger *et al.*, 1986; Eichelberger and Westrich, 1981; Jaupart, 1998; Kazahaya *et al.*, 1994; Melnik *et al.*, 2005; Papale *et al.*, 1998; Wilson *et al.*, 1980; Woods and Koyaguchi, 1994). The Sakurajima volcano is one of the best places for conducting petrological investigations of magmatic degassing processes, especially because fresh ash samples are frequently discharged by eruptions at relatively short time intervals. The volcanic activity of Sakurajima has been extensively monitored in recent years, including for example, the timing of eruptions, the height of volcanic clouds, thermal infrared imaging of the vent, SO₂ gas fluxes, volcanic earthquakes, and crustal deformation (*e.g.*, Iguchi *et al.*, 2008; Yokoo, 2009, Kazahaya *et al.*, this volume, Japan Meteorological Agency (JMA)). Here we describe temporal changes in the color and amount of leachates (Cl, F, S) absorbed on the ash. The analysis of ash leachates (Witham *et al.*, 2005) has been used in the past to estimate the composition of volcanic gases, and also in monitoring the stages of eruption of a volcano (*e.g.*, Nogami *et al.*, 2002).

In this study, the ashes were collected shortly after each eruption took place, without having exposed to rain. The analysis of the color of volcanic ash can provide information about the temperature and oxidation state of the post eruptive magma (Miyagi *et al.*, 1998; Miyagi and Tomiya, 2002; Moriizumi *et al.*, 2008; Yamanoi *et al.*, 2008).

2. Recent activity of Sakurajima

Over the past three decades, eruptions of the Sakurajima volcano occurred at the Showa crater and the Minami-dake summit crater. The current center of volcanic activity is the Showa crater (N31° 34' 43", E130° 39' 45") located about 750 m above sea level on the eastern hill of the summit of Minami-dake. Volcanic activity within the Showa crater commenced on 26 October 1939, and subsequently ceased by 1948. Since 1948, the Minami-dake summit crater has been the only active volcanic center of the Sakurajima volcano, until eventually recommencement of volcanic activity in the Showa crater took place in June 2006. On 3 February 2008, explosive eruptions began within the Showa crater. Since mid-April 2008, red-hot ejecta have been observed at night by network cameras installed around the volcano. Seemingly in response to the

*Geological Survey of Japan, Tsukuba Central 7, 1-1-1 Higashi, Tsukuba, Ibaraki 305-8567, Japan.

Corresponding author: Isoji Miyagi
e-mail: miyagi.iso14000@aist.go.jp

Table 1. List of samples.

Sample ID	Eruption		Sampling	
		vent, day, time, (height (m))	day, time, (yield (g/m ²)), location	
Skr2009 0503	S	03 09:23 (1500), 03 09:50 (500)	03 10:00-13:00	Kagoshima
Skr2009 0504	S	04 16:45 (> 2500), 4 17:58 (> 1300)	04 09:00-5 09:00	JMA
Skr2009 0804	S	03 09:00-4 09:00	03 09:00-4 09:00 (5)	JMA
Skr2009 0806	S	05 09:00-6 09:00	05 09:00-6 09:00 (8)	JMA
Skr2009 0808	S	07 19:47 (800), 08 05:02 (1000), 08 05:48 (1200)	07 09:00-8 09:00 (5)	JMA
Skr2009 0810	S	10 17:31 (1000)	09 09:00-10 09:00 (12)	JMA
Skr2009 0816	S	16 15:49 (1000)	16 16:30	Kagoshima
Skr2009 0818	S	17 09:36 (1000)	17 09:00-18 09:00 (21)	JMA
Skr2009 0819	S	19 04:25	18 09:00-19 09:00 (14)	JMA
Skr2009 0826	S	25 22:55 (1000)	25 09:00-26 09:00 (1)	JMA
Skr2009 0904	S	04 09:51 (800), 04 14:54 (800), 05 04:36, 05 05:23 (1000)	04 09:00-5 09:00 (19)	JMA
Skr2009 0911	S	11 14:09 (1000)	11 14:30	Sakurajima
Skr2009 0916	S	16 15:06 (1200)	16 09:00-17 09:00 (19)	JMA
Skr2009 0924	S	23 15:01 (1000)	23 09:00-24 09:00 (21)	JMA
Skr2009 0930	S	30 13:43 (1200)	30 14:00	Sakurajima
Skr2009 1004a, Skr2009 1004b	M	03 16:45 (3000), 04 01:19 (> 1000), 04 03:04 (> 1000)	04 Oct.	Tarumizu
Skr2009 1024	S	23 23:25 (1000)	23 09:00-24 09:00 (39)	JMA
Skr2009 1030	S	29 11:13 (1500) 29 14:38 (1300), 29 14:53 (1400), 29 16:22 (1000), 29 16:57 (1600), 29 20:07 (1800), 30 02:33 (1100), 30 03:40 (1200), 30 04:41 (1000), 30 04:58 (1600), 30 06:02 (1000), 30 06:22 (1200)	29 09:00-30 09:00 (27)	JMA
Skr2009 1118a	S	17 21:14 (> 600)	18 13:30	Tarumizu
Skr2009 1118b	S	17 21:14 (> 600)	18 13:00	Sakurajima

vigorous activity of the Showa crater, the frequency of eruptions at Minami-dake has since declined.

3. Samples

Ash samples collected from the Showa and Minami-dake summit crater from 1981 to 2009 were documented previously by Miyagi *et al.* (2010), in addition to that younger samples collected from 2009 to 2011 (Table 1) are

the subject of the present work. Ash samples in this study were collected either by the JMA or by the Geological Survey of Japan (GSJ) shortly after extrusion without having been exposed to rain, with exception of sample Skr2008 0203 (A) (Miyagi *et al.*, 2010).

4. Analysis

The chemical analyses of ash leachates (i.e., for Cl, F,

Table 1. continued.

Sample ID	Eruption		Sampling	
	vent,	day, time, (height (m))	day, time, (yield (g/m ²)),	location
Skr2009 1203	S	03 08:03 (800), 03 08:12 (700), 03 08:23 (700), 03 08:41 (800), 03 09:16 (700), 03 12:01 (> 500)	03 14:50	Sakurajima
Skr2010 0126a	S	26 12:19 (600)	26 13:00	Sakurajima
Skr2010 0126b	S	26 14:54 (700)	26 15:10	Sakurajima
Skr2010 0208	S	08 13:33 (1200) ~ 08 14:00	08 14:00	Sakurajima
Skr2010 0216	S	16 11:28 (1200)	16 11:40	Sakurajima
Skr2010 0309	S	08 09:00-9 09:00	08 09:00-9 09:00 (6)	JMA
Skr2010 0418	S	18 08:23 (1000)	18 10:00	Kagoshima
Skr2010 0426	S	26 05:26 (1800)	26 08:00	Kagoshima
Skr2010 0504	S	03 16:44 (600), 03 17:10 (600), 03 17:29 (1500), 03 18:07 (1500), 04 03:32 (> 400), 04 06:25 (2300)	03 09:00-4 09:00 (88)	JMA
Skr2010 0530	S	30 11:40 (2800)	30 14:00	Kagoshima
Skr2010 0602	S	02 14:42 (1800), 02 15:35 (1000), 02 16:00	02 17:30	Kagoshima
Skr2010 0603	S	03 14:13 (1200)	03 15:00-16:00	JMA
Skr2010 0624	S	24 15:51 (1500)	24 17:20	Sakurajima
Skr2010 0718	S	17 17:00-18 09:00	08 09:30	Kagoshima
Skr2010 0807	S	07 03:03 (800) 07 04:32 (600), 07 05:28 (800), 07 06:36 (800), 07 08:17 (800), 07 11:02 (1200)	07 16:00	Kagoshima
Skr2010 0808	S	08 01:35	08 10:00	Kagoshima
Skr2010 0822	S	21 21:15 (1000)	22 10:00	Kagoshima
Skr2010 0827	S	28 07:40 (> 200)	28 Aug.	Kagoshima
Skr2010 0829	S	29 06:29 (1200), 29 07:10 (1200), 29 08:07 (1000), 29 08:41 (800), 29 11:13 (1200)	29 Aug.	Kagoshima
Skr2010 0901	S	31 23:14 (800), 01 00:01 (600), 01 00:40 (600), 01 03:45 (600), 01 04:12 (800)	31 20:00-1 07:40	Kagoshima

and SO₄ contents) was performed by an ion chromatograph on aqueous solutions prepared as follows. The magmatic volatiles adsorbed on the surfaces of ash samples were first dissolved with deionized water. For each analysis, about 0.5 g of ash sample was sealed in a glass tube with about a fifty-fold weight of water, and then

activated for 30 minutes using an ultrasonic cleaner. The supernatant fluid was subsequently recovered about 2 hours after the ultrasonic cleaning, and was then filtered using a 0.45 μm membrane filter. The error associated with each analysis was estimated based on replicate analyses of individual samples, which yielded errors of ±7

Table 1. continued.

Sample ID	Eruption		Sampling	
		vent, day, time, (height (m))	day, time, (yield (g/m ²)), location	
Skr2010 0903C.KN	S	03 11:44 (1000) 03 12:20 (1200), 03 12:45 (> 1400), 03 16:28 (> 1000)	03 17:00	Sakurajima
Skr2010 0903a	S	02 23:57 (1000)	02 20:00-3 08:00	Kagoshima
Skr2010 0903b	S	03 20:41	02 22:00	Kagoshima
Skr2010 0904A.KN	S	03 16:28 (> 1000) 03 17:49 (> 1000), 03 18:40 (1000), 04 03:28 (1000), 04 04:14 (1200), 04 05:40 (1000), 04 06:49 (1500)	04 08:30	Sakurajima
Skr2010 0904E.KN	S	03 12:45 (> 1400), 03 16:28 (> 1000), 03 17:49 (> 1000), 03 18:40 (1000), 04 03:28 (1000), 04 04:14 (1200), 04 05:40 (1000), 04 06:49 (1500), 04 08:52 (800), 04 09:44 (600), 04 11:05 (> 800), 04 11:24 (600)	04 Sep.	Sakurajima
Skr2010 0904	S	04 03:28 (1000) 04 04:14 (1200), 04 05:40 (1000), 04 06:49 (1500)	04 Sep.	Kagoshima
Skr2011 0207	M	07 08:05 (2000)	7 Feb. (191)	Sakurajima
Skr2011 0207.NG	M	07 08:05 (2000)	07 09:00 (920)	Sakurajima
Skr2011 0506	S		05 May (34)	JMA
Skr2011 0525	S		25 May (27)	JMA
Skr2011 0526	S		26 May (17)	JMA
Skr2011 0603	S		03 Jun. (27)	JMA

% (1σ), $\pm 5\%$ (1σ) and $\pm 4\%$ (1σ) for F, Cl, and SO₄, respectively.

The color analyses were performed using a colorimeter (Minolta SPAD-503) on bulk ash samples and also on finer particles extracted via the method outlined below, in which color data are reported in a Commission internationale de l'éclairage (CIE) L*a*b* color space proposed by the CIE in 1976 (Wyszecki and Stiles, 1982). For each color analysis, bulk ash or finer particles were brought into direct contact with the window (10 mm in diameter) of the colorimeter while taking care not to expose the sensor to outside light. Each color analysis consisted of seven sets of measurements, of which the first and last were done on a standard (for quality control), and then the five unknown (sample) values were averaged and considered to represent the empirically determined color of the sample.

The finer particles of volcanic ash were extracted from the samples as follows. Each ash sample (comprising

1–30 g of material) was washed with deionized water (~300 g) in a beaker for 30 minutes in an ultrasonic cleaner. About 1 minute after the ultrasonic cleaning, each mixture was then separated by sedimentation (grain settling) through the water column into a thick bottom deposit and a thin upper part, comprising clay- to silt-sized particles suspended in water. Taking special care not to include any material from the thick bottom deposit, the upper part was decanted into an evaporating dish. The finer particles were then recovered from the suspension by overnight drying at 90°C to evaporate water from the suspension, leaving only the fine ash particles behind in the evaporating dish.

The aftermentioned thick bottom deposit was further washed, dried, sieved, and weighed to obtain the grain size distribution of the ash particles (Table 2), and these particles were then observed under a binocular microscope.

Table 2. Cumulative grain size distribution.

Sample ID	silt	< 150 μm	< 300 μm	< 710 μm	< 1 mm	> 1 mm
	(wt. %)					
Skr1981 0728-29	36.0	93.8	100.0	100.0	100.0	100.0
Skr1982 0730-31	41.0	98.9	100.0	100.0	100.0	100.0
Skr1983 0628-29	38.9	81.9	99.5	100.0	100.0	100.0
Skr1984 0603-04	26.1	54.4	90.9	100.0	100.0	100.0
Skr1986 0605-06	40.7	61.8	82.0	100.0	100.0	100.0
Skr1987 1112-13	42.9	85.1	100.0	100.0	100.0	100.0
Skr1988 0615-16	44.0	83.3	97.5	99.9	100.0	100.0
Skr1989 0824-25	45.1	67.6	97.4	100.0	100.0	100.0
Skr1990 0808-09	53.1	95.5	100.0	100.0	100.0	100.0
Skr1991 0826-27	43.8	91.7	99.9	100.0	100.0	100.0
Skr1992 0104-05	76.5	100.0	100.0	100.0	100.0	100.0
Skr2008 0203 (A)	31.3	35.7	43.8	57.6	64.3	100.0
Skr2008 0203 (B)	77.3	84.1	88.2	90.5	91.7	100.0
Skr2008 0205 (C)	69.0	82.9	94.4	99.0	99.3	100.0
Skr2008 0403	63.5	87.4	99.7	100.0	100.0	100.0
Skr2008 0404	30.8	63.3	97.4	99.8	99.8	100.0
Skr2008 0408	40.9	50.2	54.7	55.5	57.7	100.0
Skr2008 0411	51.9	100.0	100.0	100.0	100.0	100.0
Skr2008 0507	90.7	96.9	100.0	100.0	100.0	100.0
Skr2008 0508	27.1	49.2	96.5	100.0	100.0	100.0
Skr2008 0515	38.3	97.8	99.7	99.9	100.0	100.0
Skr2008 0530	41.2	70.6	100.0	100.0	100.0	100.0
Skr2008 0613	60.6	100.0	100.0	100.0	100.0	100.0
Skr2008 0705	40.9	55.5	67.0	87.5	96.0	100.0
Skr2008 0709-10	30.3	68.9	96.7	99.5	99.6	100.0
Skr2008 0728	34.9	40.3	69.7	100.0	100.0	100.0
Sample ID	silt	< 125 μm	< 250 μm	< 500 μm	< 1 mm	> 1 mm
	(wt. %)					
Skr2009 0128	42.9	59.7	93.2	100.0	100.0	100.0
Skr2009 0206a	10.7	22.0	90.2	99.9	100.0	100.0
Skr2009 0206b	48.3	68.5	84.8	100.0	100.0	100.0
Skr2009 0310a	16.6	36.1	58.9	87.1	93.6	100.0
Skr2009 0310b	22.4	41.5	62.3	76.7	90.3	100.0

5. Results

5-1 Particle size and composition

The results of grain size analysis of volcanic ash samples from this study are shown in Table 2 along with the previously characterized samples reported by Miyagi *et al.* (2010). The finer particles recovered from the liquid suspension are noted as “silt” in Table 2, and those frac-

tions generally comprised at least a few tens of wt.% of the bulk ash sample in total. All of the ash samples examined in this study are dominated by fine particles smaller than 2 ϕ (i.e., less than 0.25 mm in diameter), except for those samples originating from earlier eruptions in 2008 (i.e., Skr2008 0203(A) and Skr2008 0408).

The coarser ash particles tend to be non-vesicular, round-

Table 2. continued.

Sample ID	silt	< 125 μm	< 250 μm	< 500 μm	< 1 mm	> 1 mm
	(wt. %)					
Skr2009 0409a	34.8	41.4	51.7	85.3	99.6	100.0
Skr2009 0409b	39.4	54.6	69.7	83.6	94.1	100.0
Skr2009 0409c	47.8	66.0	95.2	99.9	99.9	100.0
Skr2009 0816	44.7	64.5	99.7	100.0	100.0	100.0
Skr2009 0911	16.4	18.7	20.2	89.5	100.0	100.0
Skr2009 1004a	3.7	5.3	18.9	99.3	100.0	100.0
Skr2009 1118a	35.0	52.7	71.3	98.1	100.0	100.0
Skr2009 1203	15.5	24.2	47.1	93.7	99.3	100.0
Skr2010 0208	52.5	83.0	93.1	99.7	100.0	100.0
Skr2010 0418	6.9	74.5	99.8	100.0	100.0	100.0
Skr2010 0426	18.4	90.1	99.9	99.9	99.9	100.0
Skr2010 0504	8.9	11.4	95.9	100.1	100.0	100.0
Skr2010 0530	23.9	98.9	99.7	99.8	100.0	100.0
Skr2010 0602	25.3	38.4	64.2	99.8	100.0	100.0
Skr2010 0603	25.0	46.9	99.6	100.0	100.0	100.0
Skr2010 0624	0.1	51.7	88.1	100.0	100.0	100.0
Skr2010 0718	27.3	55.1	93.7	100.0	100.0	100.0
Skr2010 0807	37.9	54.4	78.6	99.6	100.0	100.0
Skr2010 0808	34.0	59.5	74.7	97.9	100.0	100.0
Skr2010 0822	41.9	76.5	99.7	100.0	100.0	100.0
Skr2010 0827	44.6	67.4	88.1	99.9	100.0	100.0
Skr2010 0829	51.2	69.5	86.1	100.0	100.0	100.0
Skr2010 0901	22.3	89.7	100.0	100.0	100.0	100.0
Skr2010 0903C.KN	36.2	66.7	90.5	99.8	100.0	100.0
Skr2010 0903a	33.8	99.9	99.9	100.0	100.0	100.0
Skr2010 0903b	32.8	78.7	99.9	100.0	100.0	100.0
Skr2010 0904	34.0	48.4	84.4	100.0	100.0	100.0
Skr2010 0904A.KN	30.1	60.0	95.9	100.0	100.0	100.0
Skr2010 0904C.KN	34.2	44.6	56.3	71.6	84.0	100.0
Skr2010 0904E.KN	23.7	40.9	58.7	80.9	96.5	100.0
Skr2011 0207	44.1	79.0	90.8	92.5	99.0	100.0
Skr2011 0207.NG	33.7	46.4	87.9	100.0	100.0	100.0
Skr2011 0506	20.2	53.0	97.7	99.9	100.0	100.0
Skr2011 0525	23.6	71.4	98.7	100.0	100.0	100.0
Skr2011 0526	31.7	80.3	99.0	100.0	100.0	100.0
Skr2011 0603	16.2	99.8	100.0	100.0	100.0	100.0

ed, and are interpreted to represent recycled ash particles that were crushed long before eruption. Relative to the coarser particles, the moderate grain-size fractions exhibit surface features consistent with crushing upon eruption; *e. g.*, freshly fractured surfaces and angular grains. Fresh ash

particles are found throughout the ash deposits originating from activity of the Showa volcanic vent since February 2008. These fresh particles consist of both crystal-rich and crystal-poor varieties, with or without tiny bubbles.

Despite having freshly fractured surfaces and angular

Table 3. Amount of ash leachates (F, Cl, SO₄) and the Cl/S ratios. Data marked with asterisks are from Miyagi *et al.* (2010).

Analysis ID	F	Cl	SO ₄	Cl/S	
	(mg/kg)			(mol/mol)	
Skr1981 0729	130	900	3800	0.63	*
Skr1982 0731	62	290	960	0.82	*
Skr1983 0629	52	990	2800	0.95	*
Skr1984 0604	26	650	3200	0.55	*
Skr1986 0606	10	13	94	0.38	*
Skr1987 1113	22	98	680	0.39	*
Skr1988 0616	51	380	1500	0.68	*
Skr1989 0825	95	850	870	2.63	*
Skr1990 0809	72	690	910	2.05	*
Skr1991 0827	17	30	210	0.38	*
Skr1992 0105	160	47	1100	0.11	*
Skr2006 0614b	69	650	7900	0.23	*
Skr2006 0614c	73	660	7600	0.23	*
Skr2007 0523	110	430	9900	0.12	*
Skr2008 0203Aa	200	440	27000	0.04	*
Skr2008 0203Ab	160	360	23000	0.04	*
Skr2008 0203Ba	670	4800	43000	0.30	*
Skr2008 0203Bb	700	5000	45000	0.30	*
Skr2008 0203Ca	440	3200	31000	0.28	*
Skr2008 0203Cb	500	3400	33000	0.28	*
Skr2008 0203Cc	450	3300	31000	0.29	*
Skr2008 0403	200	1600	21000	0.20	*
Skr2008 0404	190	520	11000	0.13	*
Skr2008 0408a	110	1100	13000	0.22	*
Skr2008 0408b	110	1000	13000	0.22	*
Skr2008 0408c	110	1000	14000	0.20	*
Skr2008 0411	130	530	20000	0.07	*
Skr2008 0428	210	1200	16000	0.21	*
Skr2008 0507	120	820	14000	0.16	*
Skr2008 0508	110	390	13000	0.08	*
Skr2008 0509	110	590	21000	0.08	*
Skr2008 0515	160	900	11000	0.22	*
Skr2008 0530	74	390	12000	0.09	*
Skr2008 0603	160	670	4400	0.41	*
Skr2008 0613	40	570	15000	0.10	*
Skr2008 0705	370	1600	19000	0.24	*
Skr2008 0709	160	390	6500	0.16	*

shapes associated with post-vitrification crushing during eruption, the ash particles show various degrees of alteration, the intensity of which was estimated on the basis of observed variations in brightness of BEI/SEM images of the ash particles (Miyagi *et al.*, 2010). The ratio of altered to unaltered ash particles is high in cases where ash samples were erupted a long time after the previous eruption, and this ratio was observed to drop rapidly for samples that were erupted at short intervals (*e.g.*, figure 6a in Miyagi *et al.*, 2010). In addition, the proportion of glassy (crystal-poor) to blocky (crystal-rich) particles varied systemat-

Table 3. continued.

Analysis ID	F	Cl	SO ₄	Cl/S	
	(mg/kg)			(mol/mol)	
Skr2008 0710	87	140	6600	0.06	*
Skr2008 0728	68	220	9400	0.06	*
Skr2008 0912	640	2500	14000	0.49	*
Skr2009 0128	190	1200	9300	0.34	*
Skr2009 0202a	85	50	7600	0.02	*
Skr2009 0202b	160	830	17000	0.13	*
Skr2009 0310a	57	87	4400	0.05	
Skr2009 0310b	43	95	1800	0.15	
Skr2009 0409a	43	490	12000	0.11	
Skr2009 0409b	60	530	13000	0.11	
Skr2009 0409c	58	660	15000	0.12	
Skr2009 0503	130	660	17000	0.11	
Skr2009 0504	170	1600	25000	0.18	
Skr2009 0804	110	770	11000	0.18	
Skr2009 0806	72	530	12000	0.12	
Skr2009 0808	130	780	11000	0.18	
Skr2009 0810	13	45	720	0.17	
Skr2009 0816	38	530	14000	0.10	
Skr2009 0818	88	600	9600	0.17	
Skr2009 0819	22	37	930	0.11	
Skr2009 0826	91	530	12000	0.12	
Skr2009 0904	68	360	6500	0.15	
Skr2009 0911	57	330	9800	0.09	
Skr2009 0916	130	210	12000	0.05	
Skr2009 0924	120	450	5100	0.24	
Skr2009 0930	100	700	6000	0.32	
Skr2009 1004a	71	110	2700	0.11	
Skr2009 1004b	62	86	2700	0.09	
Skr2009 1024	10	29	590	0.13	
Skr2009 1030	66	130	6100	0.06	
Skr2009 1118a	66	820	15000	0.15	
Skr2009 1203	74	360	6200	0.16	
Skr2010 0126a	29	100	1700	0.17	
Skr2010 0126b	38	110	2100	0.14	
Skr2010 0208	86	700	13000	0.14	
Skr2010 0309	6	24	68	0.95	
Skr2010 0418	32	21	1500	0.04	
Skr2010 0426	61	300	4400	0.19	
Skr2010 0504	59	73	2900	0.07	
Skr2010 0530	51	320	8100	0.11	

ically with time, similar to the observed variation in the proportion of altered to unaltered particles. This variation in glassy/blocky constituents of ash sample is considered to reflect the faster cooling rate of magma in cases where eruption occurred through a less-heated volcanic conduit after longer repose (Miyagi *et al.*, 2010).

5-2 Water-soluble magmatic volatiles

The amount of water-soluble ions of chlorine and sulphate adsorbed onto volcanic ash particles from Sakura-

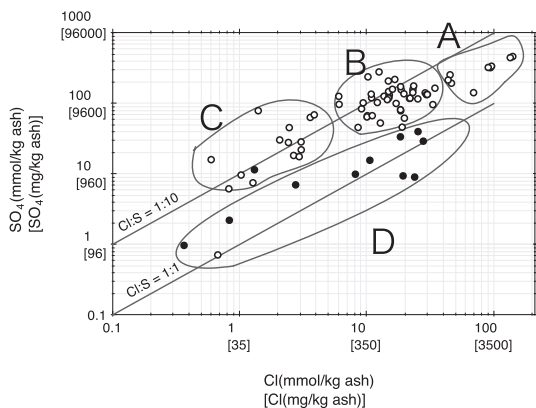


Fig. 1. Amount of water-soluble chlorine and sulphate ions (in mmol/kg ash or in mg/kg ash) adsorbed onto ash surfaces for deposits erupted during 1981–2010. Data are from Table 3 and Miyagi *et al.* (2010). Solid circles represent data collected from the Minami-dake summit vent during 1981 to 1992. Open circles represent data from the Showa volcanic vent, with the exception of one sample (Skr2008 0428) that is a mixture of ashes from the Showa and Minami-dake summit vents. Two reference lines are also shown on the plot as guide lines for examining the data—the S/Cl molar ratio of the upper reference line is 10, and for the lower reference line this value is 1.

jima eruptions during the time span of 1981–2010 ranges across three orders of magnitude (Table 3, Fig. 1). While the data for ashes from the Minami-dake summit vent for the period 1981–1992 (open circles) fall along a lower reference line (with S/Cl of ~ 1), those from the Showa volcanic vent from 2006–2010 (solid circles) have higher sulphur concentrations that plot along an upper reference line with S/Cl of ~ 10 (Fig. 1). Thus, in terms of the amount of water-soluble chlorine and sulfur, the volcanic ash samples are classified into two major groups: one with a molar S/Cl ratio of ~ 10 , and another with a molar S/Cl ratio of ~ 1 and that contains notably less sulfur (group D). The former group is subdivided into groups A, B, and C, which are ordered according to their decreasing amounts of sulfur.

There is also a documented temporal association whereby the timing of eruptions correlates with these different geochemical groupings of ash leachates (Fig. 2). For example, all ashes from the Minami-dake summit vent erupted from 1981 to 1991 belong to group D, with one outlier plotting in the group C region (Fig. 1; 5 January 1992). Ash samples from the Showa vent extruded on 6 June 2006 and before 2008 belong to group C. Samples from explosive eruptions at the Showa vent initially belong to groups A and B; i.e., in the early stages of eruption in

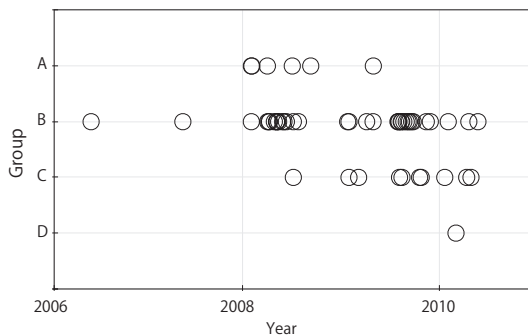


Fig. 2. Temporal changes in ash leachate compositional groups. See Fig. 1 for the grouping criteria.

2008. On 9 July 2008, however, ashes of group C reappeared. With time, the frequency of group A ashes seems to have decreased, while the frequency of group B and C ash accumulations was observed to increase with time, and finally on 9 March 2010, ashes of group D were erupted for the first time from the Showa volcanic vent. Thus, the observed temporal change in ash types from the Showa vent is C→A→B→C→D (Figs. 1 and 2).

To summarize, ash samples from the Showa volcanic vent show a temporal change in geochemical groupings defined by adsorbed water-soluble chlorine and sulfate, from group C→(longer interval)→A→B→C→D. The change in groups defined by ash leachate compositions from A→B→C reflects a decrease in the measured amount of sulphur and chlorine at a relatively constant rate, while the change from C→D is simply the result of a decrease in sulphur.

5-3 Color of the finer fraction

The colors of bulk volcanic ashes erupted from 3 May 2009 to 3 June 2011 range from $0.4 < a^* < 2.1$ and $0.5 < b^* < 5.6$, where a^* and b^* values are notations drawn from the CIE $L^*a^*b^*$ color space. The color of the finer particles (recovered from suspension noted as “silt” in Table 2) range from $1.5 < a^* < 4.2$ and $4.7 < b^* < 11.2$ (Table 4). These observations are consistent with previous reports that the variation in color of finer particles is larger than that of the bulk ash (Miyagi *et al.*, 2010). The color data determined for finer ash particles in this study are plotted on an a^*b^* plane (Fig. 3) to allow for direct comparisons with previously determined color data from ashes of the Sakurajima volcano (i.e., from eruptions between 3 February 2008 and October 2009); also plotted are relevant data from Miyagi *et al.* (2010) (Fig. 3). Since the finer ash particles show a remarkably large variation in color—and because they are the major constituent of the ash in terms of surface area—we will focus hereafter on the color of these finer ash particles in our discussions of the color data.

On the basis of color alone, the ash samples from the

Table 4. Color of volcanic ash.

Sample ID	Bulk ash			Fine particles		
	L*	a*	b*	L*	a*	b*
Skr2009 0503	42.5	0.6	2.7	n.a.	n.a.	n.a.
Skr2009 0504	47.2	1.5	4.2	n.a.	n.a.	n.a.
Skr2009 0804	45.5	1.3	3.3	n.a.	n.a.	n.a.
Skr2009 0806	48.0	1.7	4.1	n.a.	n.a.	n.a.
Skr2009 0808	48.9	1.7	4.1	n.a.	n.a.	n.a.
Skr2009 0810	49.5	1.9	3.8	n.a.	n.a.	n.a.
Skr2009 0816	53.2	1.5	3.4	62.7	2.9	6.2
Skr2009 0818	49.7	1.6	3.7	n.a.	n.a.	n.a.
Skr2009 0819	50.5	1.5	3.4	n.a.	n.a.	n.a.
Skr2009 0826	45.6	1.5	3.9	n.a.	n.a.	n.a.
Skr2009 0904	48.3	1.8	5.0	n.a.	n.a.	n.a.
Skr2009 0916	48.8	1.6	3.6	n.a.	n.a.	n.a.
Skr2009 0924	52.1	1.5	5.6	n.a.	n.a.	n.a.
Skr2009 0930	46.2	1.9	4.6	n.a.	n.a.	n.a.
Skr2009 1004b	38.9	0.8	2.0	n.a.	n.a.	n.a.
Skr2009 1024	44.2	1.6	3.9	n.a.	n.a.	n.a.
Skr2009 1030	48.8	2.1	5.3	n.a.	n.a.	n.a.
Skr2009 1118a	48.4	1.7	3.9	59.0	3.0	7.2
Skr2009 1203	47.3	1.5	3.6	58.0	2.5	6.2
Skr2010 0126b	33.0	0.4	0.5	n.a.	n.a.	n.a.
Skr2010 0208	51.6	1.3	3.8	57.0	1.7	5.4
Skr2010 0309	37.5	1.1	2.6	n.a.	n.a.	n.a.

Table 4. continued.

Sample ID	Bulk ash			Fine particles		
	L*	a*	b*	L*	a*	b*
Skr2010 0418	36.3	0.6	1.4	57.9	3.2	7.1
Skr2010 0426	44.2	1.3	3.5	62.4	3.2	7.6
Skr2010 0504	43.6	0.8	2.4	59.6	2.1	6.0
Skr2010 0530	46.7	1.6	4.4	61.5	4.2	9.3
Skr2010 0602	49.4	1.4	3.7	60.4	2.7	6.8
Skr2010 0603	47.7	0.9	2.6	62.1	1.5	4.7
Skr2010 0624	45.3	1.3	4.0	61.3	3.4	7.9
Skr2010 0718	46.1	1.4	3.8	61.2	3.1	7.6
Skr2010 0807	48.5	1.8	4.7	62.7	3.5	7.8
Skr2010 0808	48.7	1.9	4.9	63.3	3.6	8.2
Skr2010 0822	47.3	1.7	4.0	61.1	3.8	7.3
Skr2010 0827	48.7	1.7	4.7	n.a.	n.a.	n.a.
Skr2010 0829	54.9	1.7	5.0	n.a.	n.a.	n.a.
Skr2010 0901	42.2	1.2	3.3	55.6	2.9	6.9
Skr2010 0903C.KN	48.7	1.9	4.7	61.4	4.0	8.3
Skr2010 0903a	44.2	0.9	3.2	54.4	1.7	5.6
Skr2010 0903b	45.3	1.5	3.7	56.8	3.2	7.4
Skr2010 0904A.KN	44.0	1.4	3.5	57.1	3.1	6.5
Skr2010 0904E.KN	45.5	1.6	3.7	59.9	3.4	7.0
Skr2010 0904	50.4	1.7	4.9	n.a.	n.a.	n.a.
Skr2011 0207.NG	48.6	1.6	5.5	62.2	3.1	11.2
Skr2011 0506	45.2	1.2	3.6	59.9	3.4	8.9
Skr2011 0525	44.3	0.9	3.1	61.5	2.9	7.1
Skr2011 0526	44.8	1.0	4.2	55.6	2.4	7.9
Skr2011 0603	45.5	1.5	3.9	59.7	4.2	8.8

Sakurajima volcano erupted from 3 February 2008 to 3 June 2011 are classified into two groups: one that plots along the line $b^* = 2a^*$ (group R), and another defined by having $b^* > 2a^*$ (group Y). A typical example of group Y is those ashes erupted in the early days of re-activation of the Showa volcanic vent, from February to May 2008 (open circles in Fig. 3). A key feature of the group Y ashes is their yellowish color relative to the group R ashes. In order to quantify the deviation of the group Y color from the reference line defined by the color of group R ashes, we introduce a new parameter “ d ”, defined as the distance between the color data and the reference line $b^* = 2a^*$ on the a^*-b^* plane, where $d = |b^* - 2a^*|/\sqrt{5}$.

6. Discussion

6-1 Abundance and composition of ash leachates

The measured amount of water-soluble sulfur from ashes erupted during the early stages of re-activation of the Showa volcanic vent in 2008 (i.e., 44,600 mg SO_4/kg ash, Miyagi *et al.*, 2010)—along with most of the data presented in this study (table 3)—is higher than the concentration of sulfate dissolved in rhyolitic melt inclusions in phenocryst fragments within ash from the Sakurajima volcano (~ 900 mg SO_4/kg melt; Miyagi, unpublished data). This observation requires the existence of some additional source for such excess sulfur adsorbed onto the ash particles, and this might include CO_2 as the dominant magmatic gas carrier (Wallace and Gerlach, 1994), anhy-

drite decomposition during eruption (Devine *et al.*, 1984), a separate C-O-S vapor phase occurring as bubbles (Luhr *et al.*, 1984), exsolved sulfur originating from a rapid drop in sulfide solubility within the silicate melt due to magma mixing (Kress, 1997), and native sulfur deposited around volcanic fumaroles. In contrast the amount of water-soluble chlorine (Fig. 1) in these ashes is comparable to Cl concentrations observed in melt inclusions (~ 1000 mg Cl/kg melt; Miyagi, unpublished data), with the exception of those ashes erupted in the early stages of re-activation of the Showa volcanic vent in 2008. The observed change in ash group form CD outlined above, corresponds to the observed change in the amount of water-soluble sulfur from very S-rich ashes (i.e., far above S solubility values from the parent melt) to those ashes with adsorbed SO_4 values comparable to the observed SO_4 concentration in melt inclusions.

6-2 Relationships between color and ash leachate compositions

We observed a positive correlation between the d value of ash samples and the amount of ash leachates present within the ashes collected during 2008–2011 (Fig. 4). Accordingly, the samples with higher d values meet the group A ash (i.e., have a higher amount of ash leachates). Since air-oxidized andesitic volcanic ash shows a change in color along the line $b^* = 2a^*$ (Miyagi and Tomiya, 2002), the parameter d reflects the color change due to

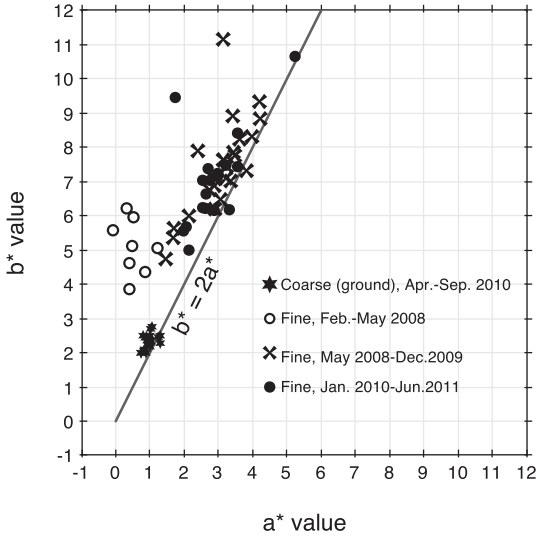


Fig. 3. Color of volcanic ashes from the Sakurajima volcano plotted on the a^* - b^* system of CIE L^* - a^* - b^* color space. The values of a^* and b^* correspond to the intensities of red ($+a^*$) and green ($-a^*$), and yellow ($+b^*$) and blue ($-b^*$) color, respectively. Open circles represent the colors of ash particles (samples erupted from eruptions that took place from February to May 2008). Crosses represent samples of volcanic ashes erupted from May 2008 to December 2009. Solid circles represent samples of volcanic ashes erupted from January 2010 to June 2011. For reference, black stars indicate the color of coarse volcanic ash particles (but ground individually via agate mortar and pestle before each color measurement) for ash samples erupted from April to September 2010. The black line represents the color variation ($b^* = 2a^*$), which indicates the general trend of colors observed in the heating experiments (of volcanic ash in air) performed by Miyagi and Tomiya (2002). This line is also nearly equal to the color variation observed in bulk-ash samples erupted from the Minami-dake summit vent during 1981–1992, and from the Showa volcanic vent from May 2008 to March 2009 (Miyagi *et al.*, 2010).

processes other than oxidation. For example, the addition of native sulfur, which has a strong yellow color ($a^*=3$, $b^*=23$), could be responsible for the color change. In fact, we observed native sulfur within the group Y ashes, the identity of which we subsequently confirmed unequivocally using X-ray diffractometry (Miyagi *et al.*, 2010). The group A ashes are characterized by minerals indicative of hydrothermal alteration, such as native sulfur, pyrite, kaolinite, gypsum, basanite, opal, and Na-alunite. These hydrothermal minerals are considered to be accumulate via fumarolic activity immediately preceding the eruption

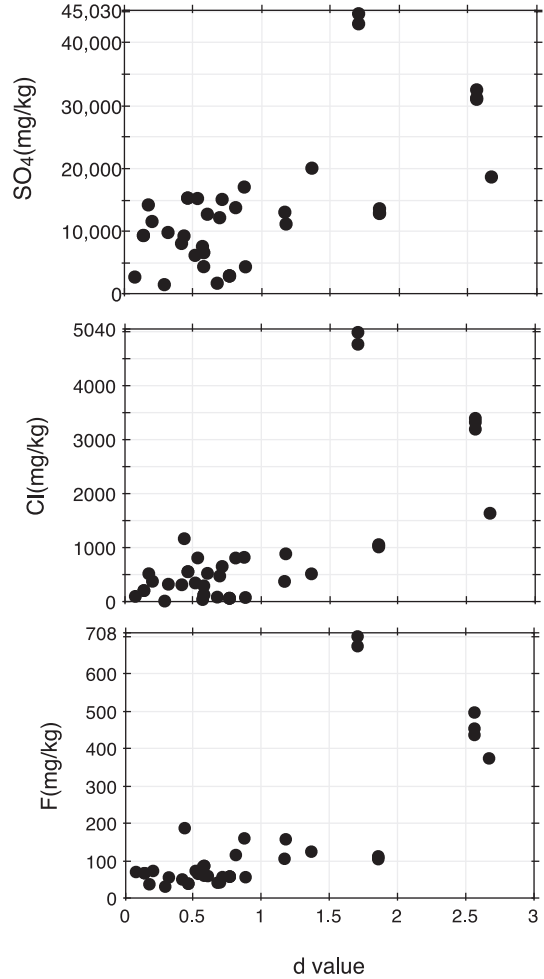


Fig. 4. Relationships between color (d value) and ash leachate compositions. The parameter d is defined as the distance on the a^* - b^* plane between the color data and for a given ash sample and the reference line $b^* = 2a^*$ on the a^* - b^* plane ($d = |b^* - 2a^*|/\sqrt{5}$).

(Miyagi *et al.*, 2010), which suggests a possible connection between the value of d and the amount of ash leachates accumulated through pre-eruptive hydrothermal alteration. The group A ashes were erupted only during the early stages of reactivation of the Showa volcanic vent in 2008 (Miyagi *et al.*, 2010), which suggests a possible control on the extent of hydrothermal alteration by the length of time between eruptions.

6-3 Links with duration of eruption intervals

The time intervals between eruptions of the Sakurajima volcano were examined in order to test whether the duration of pre-eruptive fumarolic activity affects the extent to which alteration takes place near the top of the volcanic conduit, and whether, as a consequence, this affects the ash

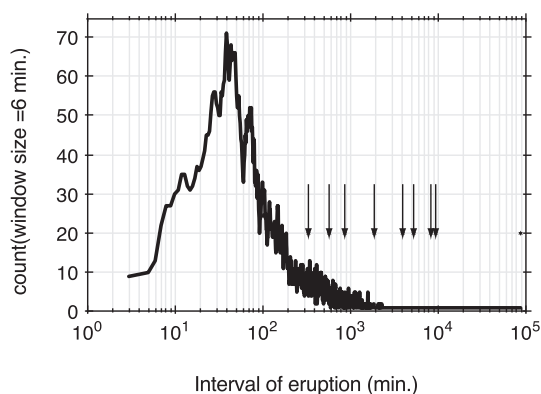


Fig. 5. Frequency plot of the durations of intervals between successive eruptions of Sakurajima volcano. Horizontal axis represents the duration of the time interval between successive eruptions, and the vertical axis represents the number of neighboring data points for a given interval duration (within ± 3 minutes, i.e., a window size of 6 minutes). The duration of the interval between successive eruptions for the group A ash samples (Fig. 1) is highlighted with arrows.

color and the amount of ash leachates extracted. Timing data for each eruption at Sakurajima —e.g., “2011/02/07 08: 05”— are drawn from the JMA website (<http://www.seisvol.kishou.go.jp>). Our eruption-interval data range from February 2008 to April 2011, with the exception of a short (3-month) gap in available data from January to March 2010. The total number of timing data on eruption activity is 1670 data points, and the intervals of time between successive eruptions ranged from 0 to 88,624 minutes. The frequency of eruption intervals of the same length of time determined from these data is shown in Fig. 5, and we observe a notable peak in eruption interval duration at about 45 minutes. The arrows shown in Fig. 5 indicate the eruption intervals for group A samples (Fig. 1). Individual arrows are located on the right side of the each peak from which it can be seen that the yellowish ash samples with higher sulfur contents are characterized by having resided throughout longer time intervals between eruptions. We also observed a positive correlation between the measured d values of ashes and the interval between successive eruptions (Fig. 6). In other words, fluctuations in d values are small when the interval between successive eruptions is short, and vice versa. We also observed similar correlations between the duration of eruptive intervals and the amount of leachates extracted from the ashes (Fig. 7). This result suggests that the amount of leachates extracted from ash sample is a reflection of the extent/duration of the pre-eruptive hydrothermal activity that affected the deposits from which they were collected.

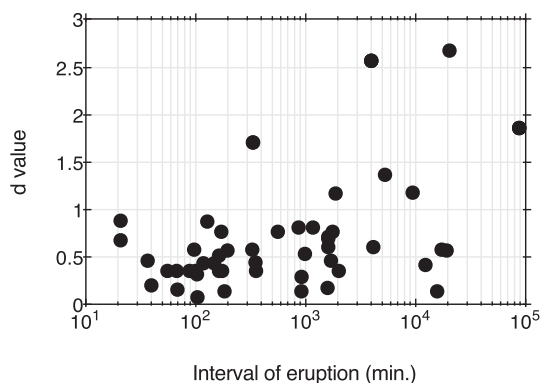


Fig. 6. Relationships between the color (d values) of volcanic ashes and the interval between successive eruptions. Some analytical results of ash samples originating from multiple eruptive events (e.g., Skr2009 0503 is a composite sample comprised of ashes erupted at 09:23 and 09:50 3 May 2009) are shown as plural spots.

6-4 Pre-eruptive hydrothermal alteration

The most important aspects of all of the above observations can be summarized as follows: (1) the amount of leachates extracted from ash sample varies by nearly three orders of magnitude over the entire range of sampled eruptions through time; (2) the amount of adsorbed ash leachates present, especially sulfur, exceeds the range of those same chemical compounds dissolved within the original melt; (3) the shorter the interval between successive eruptions, the lower the total amount of ash leachates present and the lower the d value of the ash; (4) the longer the interval between successive eruptions, the greater the range of the amount of ash leachates present and the larger the d value; and (5) the ratio of altered to the unaltered ash particles is higher in those cases where the ash deposits resided for a longer repose time before the eruption, and this ratio drops correspondingly (and rapidly) with a drop in the repose time (e.g., Fig. 6a; Miyagi *et al.*, 2010).

Fig. 8 is a schematic illustration of the cross section near the top of volcanic vent of the Sakurajima volcano. Given that a large amount of SO_2 was emitted from the Showa volcanic vent even during non-eruptive periods (i.e., 150–1880 ton/day; Kazahaya *et al.*, this volume), convective magma degassing (Kazahaya *et al.*, 1994; Shinohara *et al.*, 2003) probably taking place beneath the volcanic conduit during these times. The lower half of Fig. 8 shows an upwelling current of bubbly magma (white) and a descending current of degassed magma (black), which is essentially identical to previously proposed models of convective magma degassing (Kazahaya *et al.*, 1994; Shinohara *et al.*, 2003).

Since effective magma degassing probably only takes

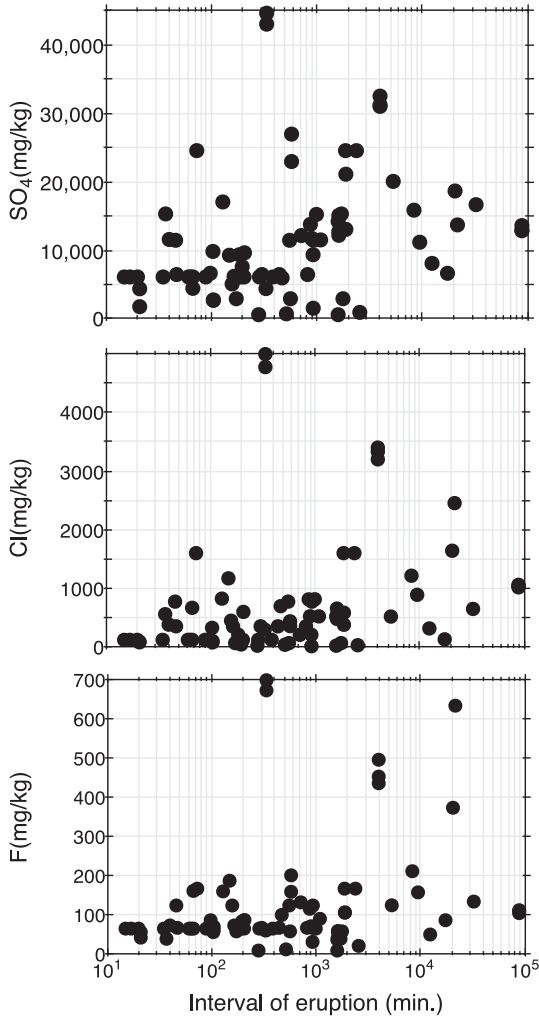


Fig. 7. Relationships between the interval between successive eruptions and the amount of ash leachates present. Some analytical results of ash samples originating from multiple eruptive events (*e.g.*, Skr2009 0503 is a composite sample comprised of ashes erupted at 09:23 and 09:50 3 May 2009) are shown as plural spots.

place after an initially impermeable porous magma suddenly turns highly permeable when the bubble fraction in the magma reaches about 80 vol.% (Takeuchi *et al.*, 2009), the productive center of magma degassing likely comprises the upper half of the diagram (Fig. 8) only (i.e., in the lower half degassing is inefficient). The upper half of this illustration depicts a complex mixture of foamy degassing magma (white) and dense degassed magma (black). It is likely that lava within the uppermost part of the diagram especially, is partly solidified and hydro-

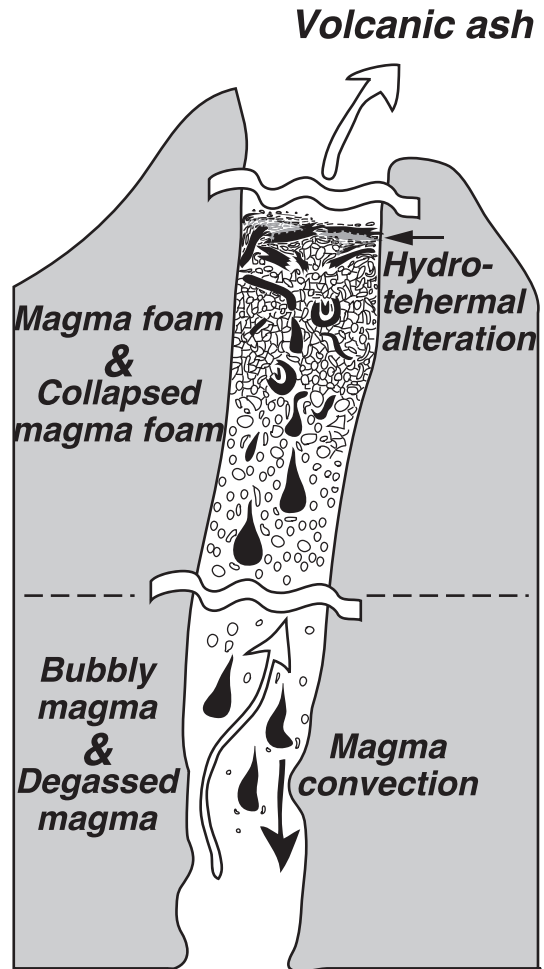


Fig. 8. A schematic cross-section near the top of volcanic vent of the Sakurajima volcano showing the distribution of pre-eruptive hydrothermal alteration. See the main text for details.

thermally altered (shaded area surrounded by dashed curve) (Fig. 8). The bubbly degassing magma originating at depth, likely becomes quite foamy through a decompression process as it reaches shallower levels, and when it ultimately collapses (degasses) while losing its form, it transforms into the dense magma that is depicted (black) in Fig. 8. As a result, the upper half of this magmatic/volcanic complex may suffer hydrothermal alteration due to extensive volcanic out-gassing, ultimately causing the excess amount of sulfur present in ash leachates. It is likely that this hydrothermally altered area is distributed heterogeneously within in the upper volcanic complex.

According to our proposed model, the observed excess sulfur in ash leachates is derived from hydrothermal or fumarolic repositories in the upper part of the volcanic

conduit, where native sulfur and/or sulfur-bearing hydrothermal minerals are deposited in and around the volcanic fumaroles. We observe that, relative to chlorine, native sulfur can become concentrated efficiently in the magmatic/volcanic complex, although we suggest that it probably then takes a substantially longer time period to replenish the sulfur repository. The longer the residence time of the magma within this upper half of the volcanic complex (i.e., the longer the eruptive interval), the greater the extent of accumulation of native sulfur in the magmatic/volcanic complex, and vice versa. Upon eruption, the upper part of the volcanic complex becomes replenished with fresh magma originating from deeper levels. The observed decrease in S/Cl (i.e., the change from group C→D ashes) probably reflects renewal of the hydrothermally altered upper part of the volcanic complex with higher S/Cl magmas relative to the S/Cl of the high-temperature volcanic gases being emitted.

7. Concluding remarks

We examined temporal changes in the color and amount of ash leachates (Cl, F, S) present within ashes erupted from the Sakurajima volcano during 1981–2011. The amount of leachates extracted from these ashes exceeded the concentration of those same chemical components dissolved within the actual melt, and varied by nearly three orders of magnitude over the eruption history studied. This variation is positively correlated with the length of time between successive eruptions, and variations in color (*d* value) of the ashes correlate with the interval between eruptions. We propose a model for this volcanic vent whereby heterogeneously distributed, eruption-renewed pre-eruptive hydrothermal alteration takes place, which ultimately explains the observed temporal changes in ash colors, and variations in abundances of adsorbed chemical species on the exterior surfaces of the ash particles.

Acknowledgments

Ash samples were collected by the JMA (Kagoshima Observatory) and by the Geological Survey of Japan (Drs. K. Nishiki and N. Geshi). Dr. R. Oikawa, Miss. T. Yamaguchi and Mrs. K. Asaoka helped with sample preparation. Constructive comments and encouragement provided by an anonymous referee, and by Drs. K. Notsu, and T. Kobayashi, improved the overall quality of the manuscript.

References

- Devine, J. D., Sigurdsson, H., Davis, A. N. and Self, S. (1984) Estimates of sulfur and chlorine yield to the atmosphere from volcanic eruptions and potential climatic effects. *J. Geophys. Res.*, **89**(B7), 6309–6325.
- Eichelberger, J. C., Carrigan, C. R., Westrich, H. R. and Price, R. H. (1986) Non-explosive silicic volcanism. *Nature*, **323**, 598–602.
- Eichelberger, J. C. and Westrich, H. R. (1981) Magmatic volatiles in explosive rhyolitic eruptions. *Geophys. Res. Lett.*, **8**, 757–760.
- Iguchi, M., Tameguri, K. and Yokoo, A. (2008) Volcanic activity of Sakurajima volcano during the period from 1997 to 2007. In *10th Joint observation of Sakurajima Volcano*, Sakurajima Volcano Research Center, 1–18 (in Japanese).
- Jaupart, C. (1998) Gas loss from magmas through conduit walls during eruption. *The Physics of Explosive Volcanic Eruptions*, **145**, 73–90.
- Kazahaya, K., Shinohara, H. and Saito, G. (1994) Excessive degassing of Izu-Oshima volcano: magma convection in a conduit. *Bull. Volcanol.*, **56**, 207–216.
- Kress, V. (1997) Magma mixing as a source for pinatubo sulphur. *Nature*, **389**, 591–593.
- Luhr, J. F., Carmichael, I. S. and Varekamp, J. C. (1984) The 1982 eruptions of el chichón volcano, chiapas, mexico: Mineralogy and petrology of the anhydrite-bearing pumices. *J. Volcanol. Geotherm. Res.*, **23**, 69–108.
- Melnik, O., Barmin, A. and Sparks, R. (2005) Dynamics of magma flow inside volcanic conduits with bubble overpressure buildup and gas loss through permeable magma. *J. Volcanol. Geotherm. Res.*, **143**, 53–68.
- Miyagi, I., Itoh, J., Shinohara, H. and Japan Meteorological Agency, Kagoshima Observatory (2010) Re-activation process of Showa volcanic vent at Sakura jima volcano in 2008: Evidence from volcanic ash. *Bull. Volcanol. Soc. Japan*, **55** (1), 21–39 (in Japanese with English abstract).
- Miyagi, I., Matsubaya, O. and Nakashima, S. (1998) Change in D/H ratio, water content and color during dehydration of hornblende. *Geochem. J.*, **32**(1), 33–48.
- Miyagi, I. and Tomiya, A. (2002) Estimation of heated temperature of volcanic ash based on the color change: An application to the landing temperature of the Miyakejima volcanic bomb ejected on 18 August, 2000. *Bull. Volcanol. Soc. Japan*, **6**, 757–761 (in Japanese with English abstract).
- Moriizumi, M., Nakashima, S., Okumura, S. and Yamanoi, Y. (2008) Color-change processes of a plinian pumice and experimental constraints of color-change kinetics in air of an obsidian. *Bull. Volcanol.*, DOI 10.1007/s00445-008-0202-5, 1–13.
- Nogami, K., Hirabayashi, J.-i., Ohba, T., Abiko, T., Okada, H., Nishimura, Y., Maekawa, T. and Suzuki, A. (2002) Geochemical monitoring of the 2000 eruption of Usu volcano –Relationship between change of water-soluble components adhering to volcanic ashes and volcanic activity–. *Bull. Volcanol. Soc. Japan*, **47**, 325–332 (in Japanese with English abstract).
- Papale, P., Neri, A. and Macedonio, G. (1998) The role of magma composition and water content in explosive eruptions 1. Conduit ascent dynamics. *J. Volcanol. Geotherm. Res.*, **87**, 75–93.
- Shinohara, H., Fukui, K., Kazahaya, K. and Saito, G. (2003) Degassing process of Miyakejima volcano: Implications of gas emission rate and melt inclusion data. In *Developments in Volcanology*, volume 5 (De Vivo, B. and Bodnar, R. J., eds.), 147–161. Elsevier.

- Takeuchi, S., Tomiya, A. and Shinohara, H. (2009) De-gassing conditions for permeable silicic magmas: Implications from decompression experiments with constant rates. *Earth Planet. Sci. Lett.*, **283**, 101-110.
- Wallace, P. J. and Gerlach, T. M. (1994) Magmatic vapor source for sulfur dioxide released during volcanic eruptions: Evidence from Mount Pinatubo. *Science*, **265**, 497-499.
- Wilson, L., Sparks, R. S. and Walker, G. P. L. (1980) Explosive volcanic eruptions - IV. The control of magma properties and conduit geometry on eruption column behavior. *Geophys. J. R. Astron. Soc.*, **63**, 117-148.
- Witham, C., Oppenheimer, C. and Horwell, C. (2005) Volcanic ash-leachates: a review and recommendations for sampling methods. *J. Volcanol. Geotherm. Res.*, **141**, 299-326.
- Woods, A. and Koyaguchi, T. (1994) Transitions between explosive and effusive volcanic eruptions. *Nature*, **370**, 641-644.
- Wyszecki, G. and Stiles, W. (1982) **Color science: Concepts and methods, quantitative data and formulae**. John Wiley & Sons, New York, 117-248.
- Yamanoi, Y., Takeuchi, S., Okumura, S., Nakashima, S. and Yokoyama, T. (2008) Color measurements of volcanic ash deposits from three different styles of summit activity at Sakurajima volcano, Japan: Conduit processes recorded in color of volcanic ash. *J. Volcanol. Geotherm. Res.*, doi: 10.1016/j.jvolgeores.2007.11.013.
- Yokoo, A. (2009) Continuous thermal monitoring of the 2008 eruptions at Showa crater of Sakurajima volcano, Japan. *Earth Planets Space*, **61**, 1345-1350.

(Editorial handling Tetsuo Kobayashi)

桜島から放出された火山灰の水溶性付着成分と色の時間変化

宮城磯治・篠原宏志・伊藤順一

火山灰の噴出を繰り返す火道上部におけるマグマ脱ガス過程を理解するため、1981～2011年の桜島の火山灰の水溶性付着成分 (Cl, F, S) と色の時間変化を調べた。水溶性付着成分量により火山灰は、S/Cl比が約10のグループとS/Cl比が約1のグループに大別できる。1981～1991年に南岳山頂火口の活発な噴火で放出された火山灰は、S/Cl比が約1のグループに属する。2008年に活動を再開した昭和火口の火山灰は、ほとんどがS/Cl比が約10のグループに属するが、時間とともに付着成分量が低下し、2010年にはS/Cl比が約1のグループも出現した。2008年に昭和火口から放出された火山灰の色調は、時間とともに黄色みが強いものから弱いものへと推移した。黄色みの強い色調は、自然硫黄（黄色）や熱水変質鉱物の存在を反映していると考えられる。火山灰の水溶性付着成分量および黄色味の強さは、その火山灰をもたらした個々の噴火前の休止時間の長さとの相関が有ることが判明した。この相関は、火道頂部に滞留しているマグマが、火山灰となって噴火する前に、滞留時間に応じ、噴気ガスの一部を蓄積したためだと思われる。1981～2011年にかけて観察された火山灰の水溶性付着成分量と色の変化は、火道内マグマ対流と噴火によるマグマの入れ替わりに対応した、火道頂部におけるマグマ平均滞留時間の変遷を反映していると解釈される。